ELSEVIER

Biochimica et Biophysica Acta 1503 (2001) 314–328

BIOCHIMICA ET BIOPHYSICA ACTA
BBA

www.elsevier.com/locate/bba

Nucleotide effects on liver and muscle mitochondrial non-phosphorylating respiration and membrane potential

Mika B. Jekabsons *, B.A. Horwitz

Section of Neurobiology, Physiology, and Behavior, Division of Biological Sciences, University of California, Davis, CA 95616, USA

Received 19 February 2000; received in revised form 28 August 2000; accepted 31 August 2000

Abstract

Uncoupling protein-1 homologs are hypothesized to mediate mitochondrial proton leak. To test this hypothesis, we determined the effects of ATP and other nucleotides on liver and skeletal muscle mitochondrial non-phosphorylating respiration (VO_2), membrane potential, FCCP-stimulated respiratory control ratios, and swelling. Neither ATP nor CTP affected liver or muscle proton leak, but both inhibited the respiratory chain. Unexpectedly, CMP stimulated liver proton leak ($EC_{50} \approx 4.4 \pm 0.5$ mM). Using CMP chromatography, we identified two proteins ($M_r = 31.2$ and 32.6 kDa) from liver mitochondria that are similar in size to members of the mitochondrial carrier protein family. We conclude (a) liver and muscle mitochondrial proton leak is insensitive to ATP and CTP, and (b) CMP activates a leak in liver mitochondria. The CMP-inducible leak may be mediated by a 30–32 kDa protein. Based on the high concentrations required, CMP is unlikely to be a physiologically important leak regulator. Nonetheless, our results show that tissues other than brown fat have inducible leaks that may be protein-mediated.

Keywords: Proton leak; Uncoupling protein; UCP2; UCP3

1. Introduction

Brown adipose tissue (BAT) mitochondria exhibit two distinct proton leaks- an inducible one mediated by uncoupling protein-1 (UCP1) and a basal one considered to be similar, if not identical, to that found in many tissues including liver and muscle [1,2]. In addition to UCP1, both uncoupling protein-2 (UCP2) and uncoupling protein-3 (UCP3) are expressed in BAT (as well as in other tissues), raising the possibility that they are responsible for the basal leak in this and other tissues. The UCP1-mediated leak, by definition, is that inhibited by purine nucleotide di- or tri-phosphates. Amino acids in UCP1 thought to participate in nucleotide binding are highly conserved in UCP2 and UCP3. Two studies have reconstituted purine nucleotide-sensitive proton and chloride transport activities from bacterially expressed UCP2 and/or UCP3 [3,4]. In contrast, three studies reported no purine nucleotide-sensitive uncoupling in isolated yeast mitochondria expressing UCP2 or 3 [5–7]. Experimental manipulation of the recombinant proteins clearly must account for these conflicting results. Thus, a different approach (and that taken in this study) is to search for nucleotide-sensitive leaks in mammalian mito-

* Corresponding author. Present address: MRC Dunn Human Nutrition Unit, MRC/Wellcome Trust Building, Hills Road, Cambridge CB2 2XY, UK. Fax: +44-1223-252805;
E-mail: mika.jekabsons@mrc-dunn.cam.ac.uk

0005-2728/01/$ – see front matter
PII: S0005-2728(00)00209-7

chondria where UCP2 and 3 are present in their native state.

The basal leak of bovine serum albumin (BSA)-treated, UCP1-deficient BAT mitochondria is insensitive to 1 mM GDP and is no different from the leak of GDP-inhibited normal BAT mitochondria despite the fact that UCP2 mRNA is up-regulated in BAT of UCP1-deficient mice [8]. Additionally, isolated muscle mitochondria from starved rats exhibit identical proton leak to fed rats despite up-regulation of UCP2 and UCP3 mRNAs and UCP3 protein [9]. These results are inconsistent with the hypothesis that UCP2 and UCP3 mediate the basal leak that is common to mitochondria from many tissues. In this study we further search for evidence of UCP2/3 involvement in proton leak by determining the effects of a variety of nucleotides on the respiration and membrane potential of skeletal muscle as well as liver mitochondria not treated with BSA.

2. Materials and methods

2.1. Animals

Male homozygous lean Zucker rats were obtained from the breeding colony at the UC Davis Animal Models Core of the Clinical Nutrition Research Unit supported by NIH. Rats were weaned at 4 weeks and housed 1–3 per cage at 20–22°C (14:10-h light/dark cycle with lights on at 06:00 h) with free access to food (stock 5012 rodent chow, Purina) and water. Rats were killed by decapitation at 12–17 weeks of age. The number of rats used for each experiment is specified in Section 3.

2.2. Reagents

Sodium salt nucleotides, oligomycin, potassium atractylate, FCCP (carbonyl cyanide *p*-(trifluoro-methoxy)phenylhydrazone), valinomycin, PMSF (phenylmethylsulfonyl fluoride), BSA (fatty acid-free bovine serum albumin), TES (*N*-tris[hydroxymethyl]-methyl-2-aminoethanesulfonic acid), rotenone, and CMP agarose were purchased from Sigma (St. Louis, MO). The voltage-sensitive dye JC-1 (5,5′,6,6′-tetrachloro-1,1′,3,3′-tetraethylbenzimidazolylcarbocyanine iodide) was purchased from Molecular Probes (Eugene, OR). Malonate and TPMP (triphenylmethylphosphonium) bromide were purchased from Aldrich (Milwaukee, WI). All other reagents were from Fisher (Santa Clara, CA).

2.3. Mitochondria isolation

Liver and hindlimb skeletal muscle (consisting of gastrocnemius, soleus, tibialis anterior, and quadriceps) were placed in cold isolation medium (containing, in mM, 250 sucrose, 50 Hepes, 10 EDTA, 1 EGTA, 0.2 PMSF, pH 7.1 at 21–23°C) and minced with surgical scissors. Tissue pieces (10–15 g) were homogenized using a Tekmar Tissumizer (Cincinnati, OH) and diluted to approximately 80 ml. To remove larger debris such as cell clumps and nuclei, homogenates were centrifuged at $750\times g$ for 15 min, then at $900\times g$ for 20 min. The resulting supernatants were decanted through two layers of cheesecloth and then centrifuged at $10\,500\times g$ for 12 min. Supernatants were aspirated and discarded, and loosely packed material was removed from the pellets by washing them (using gentle swirling) in 5 ml isolation medium. The remaining pelleted material was resuspended in approximately 40 ml isolation medium, and centrifuged at $10\,500\times g$ for 12 min. Pellets were rewashed with 5 ml of (in mM) 250 sucrose, 10 Hepes, 1 EGTA, 0.1 PMSF (pH 7.1 at 21–23°C) and resuspended in the same medium. After removal of the tissues, all isolation procedures were conducted at 0–5°C.

2.4. Oxygen consumption measurements

Aliquots of mitochondria (0.050–0.200 ml; approximately 0.2–2.5 mg protein) were pipetted into reaction buffer equilibrated to 37°C (1.84–1.69 ml) in a Gilson Oxygraph (Middleton, WI) chamber fitted with a Clark type electrode. Final concentration of reaction buffer constituents were (in mM): 120 KCl, 5 NaCl, 5 K_2HPO_4/KH_2PO_4, 2 $MgCl_2$, 0.1 Mg acetate, 50 Hepes, 5 EGTA, and 5 μM rotenone (an inhibitor of NADH oxidation by complex I of the respiratory chain). The final reaction buffer pH at 37°C was 6.90 or 7.65, depending on the experiment. This standard reaction buffer was modified for certain experiments by substitution of 2 mM $MgCl_2$ with 1 mM EDTA, or by addition of potassium

atractylate (an inhibitor of the ATP/ADP translocator; 30.3 μM final concentration). Oligomycin (solubilized in 100% ethanol) was added to a final concentration of 3.3 μg/ml and the stirred suspension was allowed to equilibrate for 3–5 min prior to addition of 5.1 mM succinate (final concentration).

Basal non-phosphorylating oxygen consumption was measured for 2–5 min, and followed by serial additions of a freshly prepared nucleotide solution. Nucleotide additions (2–10 μl each of a 0.8 M stock) were 1–4 min apart, depending on the initial respiratory rate. Changes in respiratory rates induced by nucleotides usually occurred within 20 s of the addition. For each preparation, the order of addition of the different nucleotides was rotated to minimize any possible effect of time.

Recording protocols lasted up to 6 h. Storing mitochondria on ice over this period of time did not significantly affect basal rates of non-phosphorylating respiration (liver mitochondrial respiration averaged 20.1 ± 2.8 vs. 20.1 ± 2.5 nmol O_2/(min per mg protein), immediately after isolation vs. final measurement 5–6 h later, respectively; skeletal muscle mitochondrial respiration was 87.5 ± 4.6 vs. 90.3 ± 7.8 nmol O_2/(min per mg protein), initial vs. final, respectively).

Respiratory rates were calculated from the chart recordings using an oxygen solubility coefficient of 0.02273 ml O_2/ml buffer at 37°C and 1 atm pressure [10]. The concentration of dissolved oxygen in the reaction buffer equilibrated with room air at 37°C was calculated to be 175.4 nmol O_2/ml. Aliquots of each mitochondrial preparation were stored at −20°C for later determination of protein concentration using the BCA protein assay (Pierce, Rockford, IL), with BSA as standard.

2.5. Fluorescence measurements

Mitochondria (0.070–0.100 ml; approximately 0.2–0.6 mg protein) were added to a cuvette containing prewarmed reaction buffer (37°C; 1.82–1.79 ml) prepared as for the oxygen consumption measurements. Oligomycin and the voltage-sensitive dye JC-1 (solubilized in dimethylsulfoxide) were added to final concentrations of 3.3 μg/ml and 0.47 μM, respectively. The stirred suspension was allowed to equilibrate for 6 min in a 37°C controlled Perkin–Elmer LS-5 fluorescence spectrophotometer (Foster City, CA). Excitation was set at 490 nm and emissions were recorded at 590 nm. After recording the fluorescence (in arbitrary fluorescence units, or FU), succinate was added to a final concentration of 5.1 mM. Basal non-phosphorylating fluorescence was recorded 3 min later, at which time serial additions of a freshly prepared nucleotide solution were initiated. Additions were made at 2-min intervals, with the fluorescence value recorded just prior to the next addition. Upon addition of succinate, fluorescence typically increased 2–3-fold for liver mitochondria and 3–4-fold for skeletal muscle mitochondria. FCCP (a protonophore; 0.5 μM) immediately caused both liver and skeletal muscle mitochondrial fluorescence to decrease close to the fluorescence recorded prior to succinate addition. Background JC-1 fluorescence in buffer was not affected by pH. This background fluorescence was subtracted from the pre-succinate mitochondrial fluorescence to obtain an estimate of the zero potential for the mitochondria. For liver, these values averaged 14.5 ± 1.2 FU/mg at pH 6.9, and 16.7 ± 1.6 FU/mg at pH 7.65. For skeletal muscle, these values averaged 29.3 ± 2.1 FU/mg at pH 6.9, and 45.4 ± 2.3 FU/mg at pH 7.65. For each preparation, the zero potential estimate was subtracted from all post-succinate values. JC-1 fluorescence correlates linearly to inner mitochondrial membrane potentials ranging from 20 to 200 mV [11].

2.6. TPMP measurements

TPMP-sensitive electrodes (courtesy of Martin Brand, MRC Dunn Human Nutrition Unit, Cambridge, UK) were calibrated in the standard reaction buffer at 37°C by 4–5 additions of TPMP, resulting in a final concentration of 0.68–1.2 μM. Following addition of mitochondria (0.6–2.5 mg protein) and oligomycin (3 μg/ml), the recordings were allowed to stabilize 8–10 min, at which time succinate was added to 5 mM. Upon recording a new steady-state concentration of TPMP (within 2.5 min of succinate addition), mitochondria were titrated with malonate (final concentrations 0.26, 0.52, 1.0, 2.1, 5.1, and 11.3 mM for liver and 0.26, 0.77, 1.8, 4.9, and 11.0 mM for muscle) at 1.5–3-min intervals. Addition of 0.1 μM FCCP was performed to ensure complete

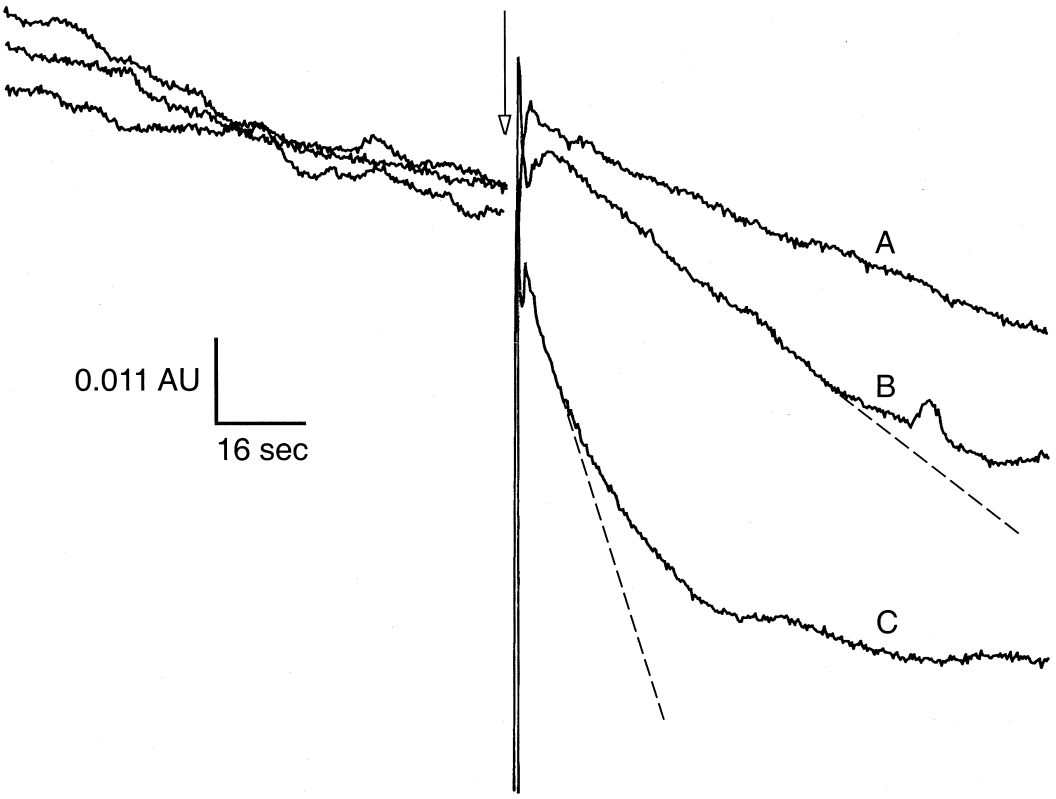

Fig. 1. Mitochondrial swelling induced by 5 nM (A), 50 nM (B), and 500 nM (C) FCCP. Isolated skeletal muscle mitochondria (0.1 ml; approximately 0.5 mg protein) were incubated at 21–23°C in the standard swelling medium (0.9 ml). Swelling was monitored by recording the decrease in absorbance units (AU) at 520 nm over 3 min. Spectrophotometric data were acquired every 0.3 s. Basal swelling was recorded for 90 s following addition of valinomycin to 0.5 μM. Recordings were briefly interrupted for addition of FCCP (indicated by the arrow). The heavy vertical lines just after the arrow are artifacts of the addition. Because the magnitude of the swelling rate was increased by higher concentrations of FCCP, the time over which linearity was maintained decreased. Dashed lines represent hand drawn extensions of the initial linear rates. Each tracing represents data collected from different aliquots of the same mitochondrial preparation.

dissipation of the membrane potential so that electrode drift could be assessed. Drift over the recording period was assumed to be linear. Membrane potentials were calculated using the Nernst equation, assuming a matrix volume of 0.6 μl/mg protein and a TPMP-binding correction factor of 0.4 [12,13]. Oxygen consumption recordings were performed in parallel as described above, except that TPMP was also included in the buffer.

2.7. Swelling measurements

Mitochondria were prepared as described in the isolation procedures, but the final pellet was resuspended in (mM) 250 sucrose, 1 EGTA, and 0.1 PMSF. Swelling rates were determined as previously described [14]. Mitochondria (0.1 ml; approximately 0.4–0.7 mg protein) were suspended in 0.9 ml of swelling buffer containing (final concentrations) 100 mM K acetate, 5 mM TES, 5 μM rotenone, and 32 μM (0.2%) fatty acid-free BSA. Swelling buffer pH was adjusted to 6.90 or 7.65 at 21–23°C with 0.5 M KOH prior to addition of mitochondria. The potassium ionophore valinomycin (solubilized in 100% ethanol) was added to 0.5 μM, and basal swelling rates were recorded for 90 s. At this time 10 μl of CMP or AMP was rapidly mixed into the cuvette and the swelling rate was recorded for an additional 90 s. Final concentrations of nucleotides used in these experiments were (in mM) 0.2, 2.5, 4.0, and 8.3. Control experiments were carried out for each preparation using FCCP added to 5, 50, and 500

nM. Linearity of induced swelling rates generally lasted from 5–60 s, depending on the magnitude of the initial swelling (Fig. 1). Swelling rates were measured as the decrease in absorbance units at 520 nm. Data were collected at 21–23°C using a Gilford System 2600 spectrophotometer (Oberlin, OH) set to acquire readings every 0.3 s. Results were displayed using a Hewlett–Packard (Palo Alto, CA) 7225B plotter.

2.8. CMP chromatography

Mitochondria were isolated from two 48-h fasted rats as described above, except that the final pellet was rinsed in (mM): 120 KCl, 5 NaCl, 5 KH_2PO_4/K_2HPO_4, 2 EDTA, 1 EGTA, 0.1 Mg acetate, 50 Hepes, pH 6.90. Pellets were gently resuspended in 1.3 ml of the same buffer containing 4% Triton X-100, and the solubilization was allowed to proceed for 45 min on ice. Unsolubilized material was pelleted by centrifugation at $100\,000 \times g$ for 30 min. The supernatant was incubated overnight with stirring at 6°C with approximately 3 μmol of CMP resin equilibrated in 0.5 ml of the same buffer without Triton X-100. The resins were washed eleven times (liver), or ten times (skeletal muscle) with the salt content of the washes reduced such that the final washes were carried out in 10 mM Hepes (pH 6.9) and 1 mM EDTA. All washes were performed at 4°C for 15 min, except the final 60-min wash. The final wash was followed with a CMP specific elution by incubating the resin for 60 min in 10 mM Hepes (pH 6.9), 1 mM EDTA, and 50 μmol CMP. This was followed with a 60 min non-specific elution in 0.8 M NaCl, 50 mM Hepes, pH 8.1. Samples were washed and concentrated using Microcon-10 microconcentrators (Amicon, Beverly, MA). One third of the final concentrated sample was electrophoresed through a denaturing 12% polyacrylamide gel. Gels were stained using BioRad's Silver Stain Plus kit (Hercules, CA).

2.9. Northern blot and reverse transcriptase–polymerase chain reaction (RT–PCR) analysis

Total RNA was extracted in Trizol reagent (Gibco-BRL, Gaithersburg, MD). Twenty μg of total RNA from each tissue was electrophoresed through a 1% agarose gel containing 2.2 M formaldehyde and $1\times$MOPS buffer. Ethidium bromide was included in each sample so that RNA integrity and equal loading could be verified. RNA was transferred and then cross-linked to Duralon-UV nylon membranes (Stratagene, La Jolla, CA). Rat UCP2 and UCP3 cDNA inserts, kind gifts from J. Granneman, Wayne State University, were excised from plasmids by *Eco*RI digestion and gel-purified using the Qiaquick gel extraction kit (Qiagen, Santa Clarita, CA). Purified cDNA was random-primed with alpha [^{32}P]dCTP (Rediprime kit, Amersham, Buckinghamshire, UK). Blots were prehybridized for 30 min in Express Hyb solution (Clonetech, Palo Alto, CA) at 68°C, and hybridized for 60 min at 68°C with ^{32}P-labeled cDNA probe (2×10^6 cpm/ml). Blots were washed twice in $2\times$SSC, 0.05% SDS at room temperature, and twice in $0.1\times$ SSC, 0.01% sodium dodecyl sulfate (SDS) at 60–65°C. Blots were exposed to X-ray film with intensifying screens for up to 2 days at −80°C.

For RT–PCR analysis, 20 μg of total RNA was treated with DNase1 according to the manufacturer's instructions (Gibco-BRL). One μg of DNase1-treated RNA was reverse transcribed using oligo dT primers (Superscript Preamplification System, Gibco-BRL). Rat UCP2-specific primers were designed from the GenBank cDNA sequence (accession no. AB010743; forward primer: 5′-GCAGCTTTGAAGAACGAG-3′; reverse primer: 5′-ATGGTCAGGGCACAGTG-3′; 953 bp product). Amplification of the housekeeping gene glyceraldehyde-3-phosphate dehydrogenase was performed on the same samples as control for the efficiency of the reverse transcription step (GenBank accession no. X02231; forward primer: 5′-TCCACCACCCTGTTGCTGTAG-3′; reverse primer: 5′-GACCACAGTCCATGCCATCACT-3′; 453 bp product). Absence of contaminating genomic DNA in the reactions was verified by running parallel PCR reactions in which reverse transcriptase was omitted from the initial step.

2.10. Statistics

Statistical analyses are as described in the figure legends and text, with the significance level set at $P \leq 0.05$. Statistics were computed by analysis of variance (ANOVA) using Super ANOVA (Abacus Con-

cepts, Berkeley, CA) and Statview (Abacus Concepts, Berkeley, CA) software for the Macintosh.

3. Results

3.1. Effects of nucleotide titrations on respiration and JC-1 fluorescence

Nucleotide-induced changes in non-phosphorylating respiration can be the result of changes in proton leak or respiratory chain activity. The two mechanisms may be distinguished from each other by determining the effects of nucleotides on the inner mitochondrial membrane potential ($\Delta\Psi$), which can be measured with the voltage-sensitive dye JC-1. If a nucleotide inhibits proton leak without directly affecting the respiratory chain, then $\Delta\Psi$ increases and, as a result, respiratory chain activity decreases as proton pumping by the chain becomes less energetically favorable [15]. Conversely, if a nucleotide activates proton leak without directly affecting the respiratory chain, then $\Delta\Psi$ falls and respiratory chain activity increases. If a nucleotide affects the respiratory chain without directly affecting proton leak, then changes in $\Delta\Psi$ follow changes in respiration. Using JC-1 as an indicator of membrane potential, an increase in $\Delta\Psi$ results in increased fluorescence while a decrease in $\Delta\Psi$ results in decreased fluorescence.

Liver mitochondrial respiration and JC-1 fluorescence were significantly inhibited by ATP and CTP at pH 6.9 (Fig. 2). These effects were reduced at pH 7.65 (Table 1). ADP and AMP had progressively less effect on liver mitochondria (Table 1 and Fig. 2). GTP and GDP had no significant effect on liver mitochondrial respiration (Table 1). The inhibitory effect of ATP persisted when 30 μM atractyloside was

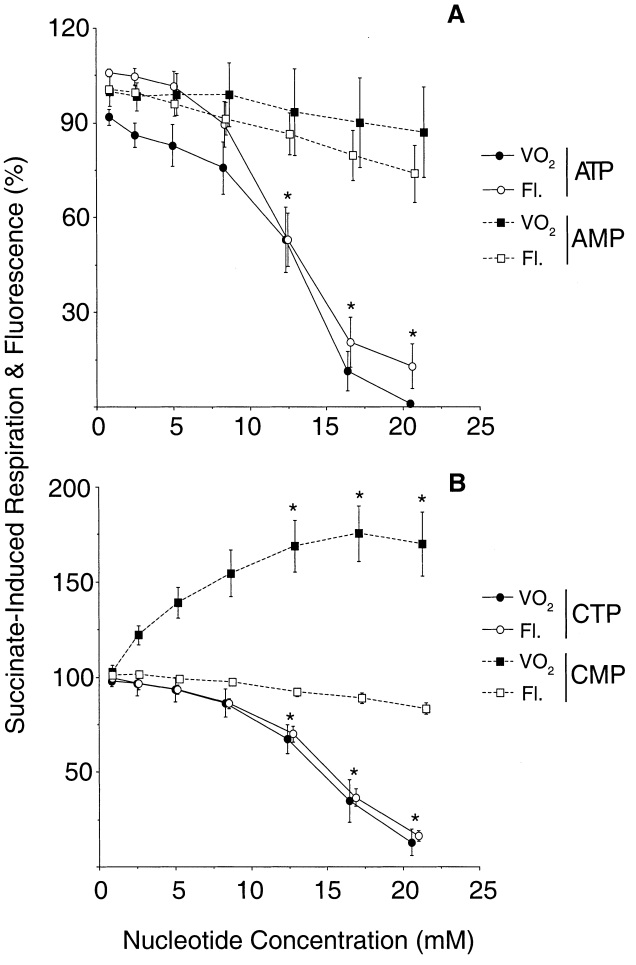

→

Fig. 2. Effects of adenine (A) and cytidine (B) nucleotides on isolated liver mitochondrial non-phosphorylating respiration (VO_2) and JC-1 fluorescence (FI) at pH 6.90. Isolated liver mitochondria were incubated at 37°C in a standard reaction buffer (see Section 2) containing 3.3 μg/ml oligomycin. For fluorescence measurements, 0.47 μM JC-1 was included. Respiration measurements were made in a Gilson Oxygraph chamber using a Clark type electrode. Fluorescence measurements were made in a cuvette using a Perkin–Elmer LS-5 fluorescence spectrophotometer (excitation 490 nm; emission 590 nm). Buffer pH at 37°C was determined for each experiment and did not vary from 6.90 by more than 0.03 pH units. Dose responses were performed by serial additions (2, 4, 6, 8, 10, 10, and 10 μl) of a freshly prepared stock nucleotide solution (approx. 0.8 M). Data are expressed as a percentage of basal respiration and fluorescence. Prior to nucleotide addition, basal respiration for ATP, AMP, CTP, and CMP curves was 17.6 ± 1.5, 17.9 ± 1.6, 19.6 ± 2.7, and 15.7 ± 1.9 nmol O_2/(min per mg), respectively. Basal fluorescence readings for ATP, AMP, CTP, and CMP curves were 34.0 ± 4.8, 31.3 ± 3.4, 32.7 ± 5.5, and 31.2 ± 3.1 FU/mg, respectively. Respiration data are mean ± S.E.M. of eight rats, except for CMP and AMP dose responses, where $n = 6$. Fluorescence data are mean ± S.E.M. of six rats (CMP), five rats (AMP), or three rats (ATP, CTP). Points without error bars indicate S.E.M. was smaller than the symbol. Two-way ANOVA (concentration and preparation) on the untransformed data was used to determine significant concentration effects. Dunnet's post hoc test was used to determine which means were significantly different from basal values. For a given nucleotide, asterisks denote concentrations at which both VO_2 and fluorescence are significantly different from basal.

Table 1
Effects of pH and magnesium ions on nucleotide regulation of liver mitochondrial non-phosphorylating respiration

Addition	pH 6.9+Mg	pH 6.9−Mg	pH 7.65+Mg	pH 7.65−Mg
None	17.3 ± 1.3	16.7 ± 1.1	22.2 ± 1.6	41.1 ± 3.2
ATP	9.8 ± 2.5[a]	0.1 ± 0.1[a]	16.7 ± 1.5[a]	14.4 ± 1.8[a]
ADP	15.5 ± 2.8	n.d.	17.2 ± 2.3	n.d.
AMP	16.5 ± 3.0	n.d.	22.5 ± 2.7	n.d.
CTP	13.3 ± 2.4	n.d.	18.6 ± 1.6	n.d.
CMP	25.8 ± 2.2[a]	n.d.	27.4 ± 2.2[a]	n.d.
GTP	18.7 ± 2.9	n.d.	n.d.	n.d.
GDP	17.4 ± 3.2	n.d.	n.d.	n.d.
Atractyloside	12.9 ± 1.2	n.d.	n.d.	n.d.
ATP+atractyloside	2.9 ± 1.3[a]	n.d.	n.d.	n.d.
ADP+atractyloside	8.7 ± 1.0[a]	n.d.	n.d.	n.d.

Data are mean ± S.E.M. of 5–8 preparations. Mitochondria were incubated at 37°C in reaction buffer equilibrated to pH 6.9 or 7.65 containing either 2 mM $MgCl_2$ (+Mg) or 1 mM EDTA (−Mg). Atractyloside was added to 30 μM. Respiration (in nmol O_2/(min per mg protein)) was measured as described in Section 2. Nucleotide additions were as described in Fig. 2, but only 12-mM concentrations are shown. Data within a column were analyzed by one-way ANOVA using Fisher's LSD post hoc test, or *t*-test. n.d., not determined.

[a]Values within a column which are significantly different from respiration with no addition. At pH 6.9, the ATP IC_{50} was significantly lower without versus with Mg (2.3 ± 0.5 vs. 11.0 ± 1.4 mM; *t*-test).

included in the reaction buffer (Table 1). In contrast, CMP significantly increased respiration (peak increase of 11.0 nmol O_2/(min per mg protein), or 75% at 17.1 mM CMP) while JC-1 fluorescence was reduced significantly (3.5 FU/mg, or 11% at peak respiratory response; Fig. 2). The CMP concentration that yielded half-maximal respiratory stimulation was determined to be 4.4 ± 0.5 mM. This effect was attenuated at pH 7.65 (Table 1).

Similar trends were seen with skeletal muscle mitochondria - ATP and CTP had the greatest inhibitory effects on respiration and fluorescence while ADP and AMP had progressively smaller effects (Table 2 and Fig. 3). The inhibitory effects of ATP and

Table 2
Effects of pH and magnesium ions on nucleotide regulation of muscle mitochondrial non-phosphorylating respiration

Addition	pH 6.9+Mg	pH 6.9−Mg	pH 7.65+Mg	pH 7.65−Mg
None	93.6 ± 3.6	108.5 ± 4.1	81.3 ± 2.8	102.3 ± 6.4
ATP	45.4 ± 9.3[a]	18.8 ± 5.9[a]	102.8 ± 2.4[a]	85.0 ± 5.2
ADP	63.5 ± 6.8[a]	n.d.	102.6 ± 2.0[a]	n.d.
AMP	73.6 ± 8.3[a]	n.d.	97.0 ± 3.1[a]	n.d.
CTP	58.4 ± 6.9[a]	n.d.	95.3 ± 1.8[a]	n.d.
CMP	112.2 ± 5.2[a]	n.d.	103.9 ± 3.1[a]	n.d.
GTP	88.1 ± 7.8	n.d.	n.d.	n.d.
GDP	82.3 ± 8.4	n.d.	n.d.	n.d.
Atractyloside	98.6 ± 6.1	n.d.	n.d.	n.d.
ATP+atractyloside	65.9 ± 3.4[a]	n.d.	n.d.	n.d.
ADP+atractyloside	82.6 ± 2.9	n.d.	n.d.	n.d.

Data are mean ± S.E.M. of 5–8 preparations. Mitochondria were incubated at 37°C in reaction buffer equilibrated to pH 6.9 or 7.65 containing either 2 mM $MgCl_2$ (+Mg) or 1 mM EDTA (−Mg). Atractyloside was added to 30 μM. Respiration (in nmol O_2/(min per mg protein)) was measured as described in Section 2. Nucleotide additions were as described in Fig. 2, but only 12-mM concentrations are shown. Data within a column were analyzed by one-way ANOVA using Fisher's LSD post hoc test, or *t*-test. n.d., not determined.

[a]Values within a column which are significantly different from respiration with no addition. At pH 6.9, the ATP IC_{50} was significantly lower without versus with Mg (6.4 ± 1.0 vs. 11.2 ± 1.3 mM; *t*-test).

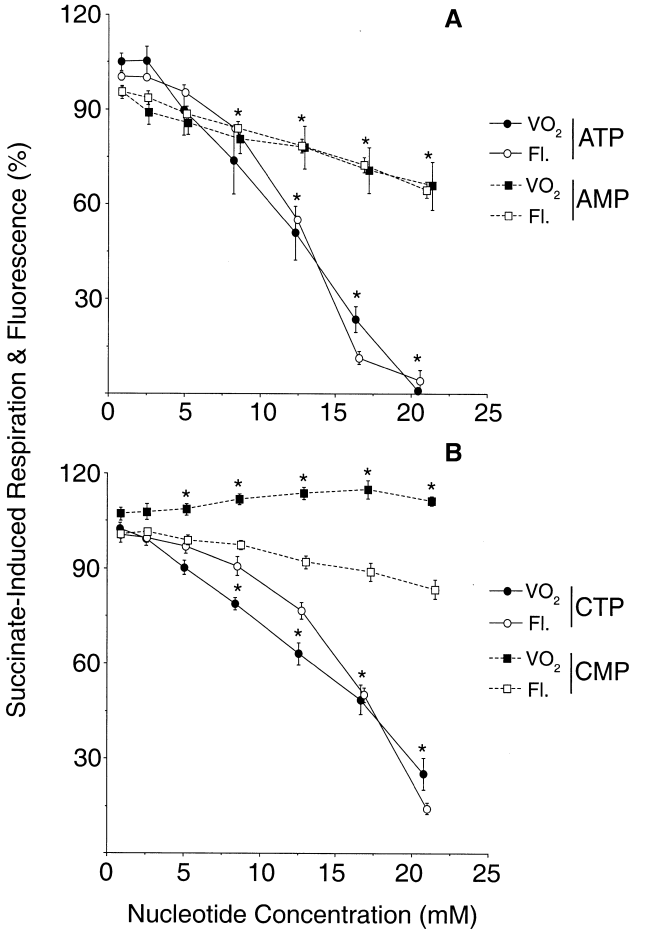

Fig. 3. Effects of adenine (A) and cytidine (B) nucleotides on isolated skeletal muscle mitochondrial non-phosphorylating respiration (VO_2) and JC-1 fluorescence (FI) at pH 6.90. Experimental setup and conditions were as described for Fig. 2. Data are expressed as a percentage of basal respiration and fluorescence. Prior to nucleotide addition, basal respiration for ATP, AMP, CTP, and CMP curves was 83.0 ± 7.5, 93.4 ± 7.4, 95.0 ± 5.2, and 98.7 ± 4.6 nmol O_2/(min per mg), respectively. Basal fluorescence readings for ATP, AMP, CTP, and CMP curves were 187 ± 30, 154 ± 18, 160 ± 8, and 147 ± 5 FU/mg, respectively. Respiration data are mean ± S.E.M. of eight rats (ATP), seven rats (CTP), or six rats (CMP, AMP). Fluorescence data are mean ± S.E.M. of six rats (AMP, CMP) or three rats (ATP, CTP). Points without error bars indicate S.E.M. was smaller than the symbol. Statistical analysis was as described for Fig. 2. For a given nucleotide, asterisks denote concentrations at which both VO_2 and fluorescence are significantly different from basal.

CTP were abolished at pH 7.65 (Table 2). GTP and GDP had relatively little effect on respiration (Table 2). As with liver, the inhibitory effects of ATP and ADP persisted in the presence of 30 μM atractyloside

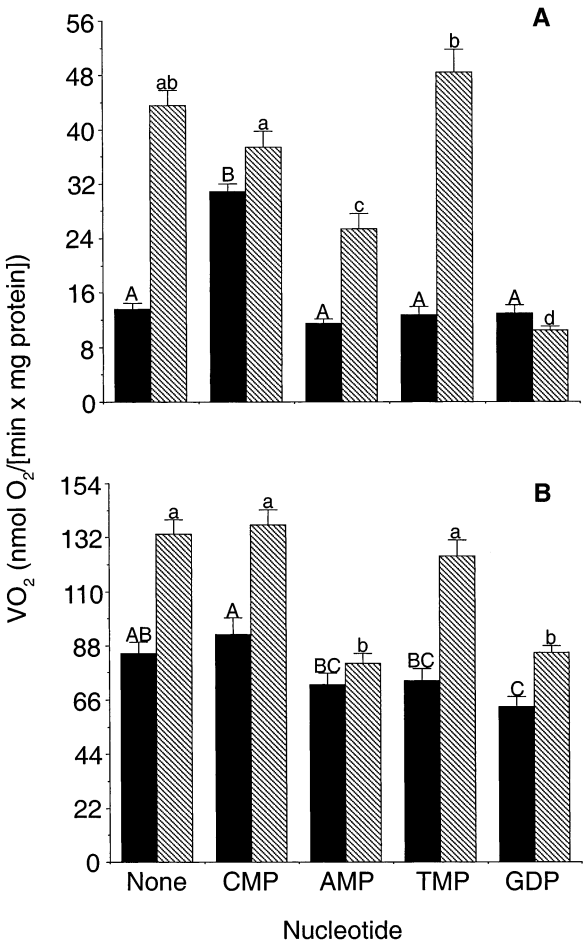

Fig. 4. Effects of nucleotide pre-incubation on basal and FCCP-stimulated non-phosphorylating respiration (VO_2) of liver (A) and skeletal muscle (B) mitochondria. Mitochondria were pre-incubated at 37°C with 12 mM nucleotide for 6 min. Upon addition of 5 mM succinate, basal VO_2 (solid bars) was measured over 14 min, at which time 70 nM (liver) or 20 nM (muscle) FCCP was added (hatched bars). Preliminary experiments were conducted to determine the concentrations of FCCP that gave the highest respiratory control ratio (RCR). The pmol FCCP added per mg mitochondrial protein ranged from 186–283 for liver and 315–414 for muscle. Data are mean ± S.E.M. of five different preparations. Data for basal and FCCP-stimulated VO_2 were analyzed separately by one-way ANOVA. Significant effects were followed by Fisher's protected LSD post hoc test to determine which means differed. Within a group, means sharing common letters (uppercase for basal and lowercase for FCCP VO_2) do not differ. Respiratory control ratio for each nucleotide was calculated as the FCCP-stimulated VO_2/basal VO_2. Liver RCRs were 3.25 ± 0.23^{a}, 1.21 ± 0.08^{b}, 2.23 ± 0.21^{c}, 3.87 ± 0.31^{d}, and 0.86 ± 0.14^{b} for no addition, CMP, AMP, TMP, and GDP, respectively. Muscle RCRs were 1.57 ± 0.03^{ab}, 1.49 ± 0.06^{ad}, 1.13 ± 0.02^{c}, 1.69 ± 0.04^{b}, and 1.36 ± 0.07^{d}. For RCR data, means sharing common superscripts do not differ.

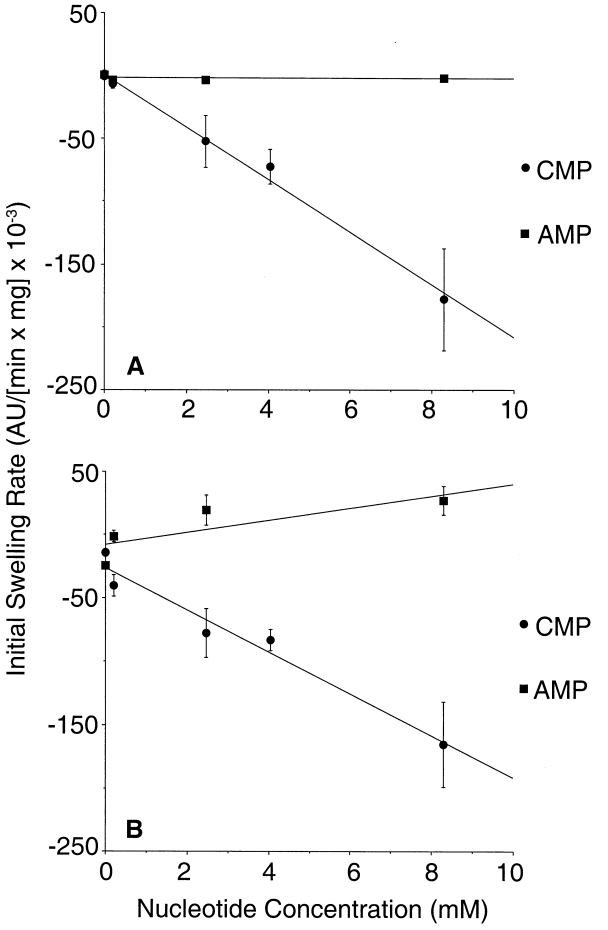

Fig. 5. Effects of CMP and AMP on liver (A) and skeletal muscle (B) mitochondrial swelling. Experiments were conducted as described in Fig. 1. Negative rates reflect decreasing absorbance units (AU) and indicate swelling of the mitochondria. Data are mean ± S.E.M. of three preparations. Points without error bars indicate S.E.M. is smaller than the symbol. Linear regression was used to fit lines to the data.

(Table 2). Respiration significantly increased with CMP titrations (Table 2 and Fig. 3). At the peak increase in muscle respiration, fluorescence was significantly reduced (−24.5 FU/mg, or 16%; Fig. 3).

Experiments with ATP were repeated with buffer in which 1 mM EDTA was substituted for 2 mM $MgCl_2$ to determine if the inhibitory effects of ATP were due to chelation of Mg. In buffer lacking Mg, ATP had a significantly greater potency than in the presence of 2 mM $MgCl_2$ (Tables 1 and 2). Furthermore, the attenuated ATP inhibition at pH 7.65 was completely reversed in liver and partially reversed in muscle by $MgCl_2$ removal (Tables 1 and 2).

3.2. *Effects of nucleotide pre-incubation on respiration and respiratory control ratios (RCR)*

From the above results, we predicted that liver and muscle mitochondria pre-incubated with CMP would exhibit lower RCR values (entirely because of increased basal non-phosphorylating respiration) than would mitochondria pre-incubated with nucleotides that had little to no affect on basal respiration (e.g., GDP, AMP). As shown in Fig. 4, this was

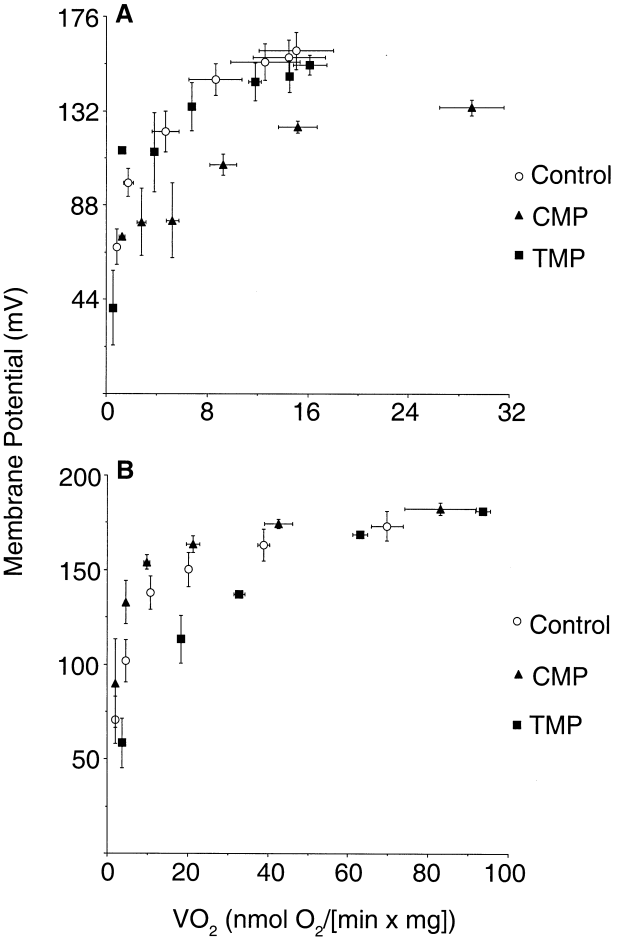

Fig. 6. Effects of CMP and TMP on liver (A) and skeletal muscle (B) proton leak kinetics. The respiratory chain of succinate-energized mitochondria with either no addition or 12 mM CMP or TMP (8 min pre-incubation) was inhibited with malonate titrations. Membrane potentials were calculated from the distribution of TPMP within and outside the mitochondrial matrix as described in Section 2 and plotted as a function of respiration (VO_2). For liver, data are mean ± S.E.M. of three (control, CMP) or two (TMP) preparations. For muscle, data are mean ± S.E.M. of five (control, CMP) or two (TMP) preparations.

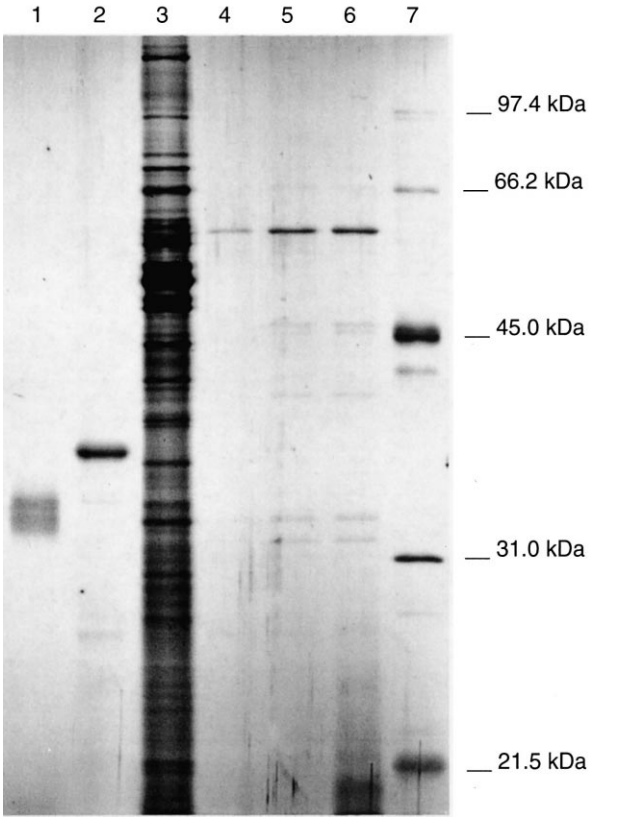

Fig. 7. SDS–polyacrylamide gel electrophoresis (PAGE) analysis of solubilized liver mitochondrial proteins prior to and following batch CMP-agarose chromatography. Solubilized liver mitochondrial proteins were incubated with stirring overnight at 6°C with approximately 3 μmol CMP immobilized to an agarose matrix. The resin was washed 11 times and eluted using 50 μmol CMP. This was followed with a non-specific elution using 0.8 M NaCl at pH 8. Samples were washed/desalted and spin-concentrated. One third of the final volume was electrophoresed through a 4% stacking and 12% resolving gel then silver stained. Lanes: 1, isolated rat UCP1; 2, purified recombinant human UCP2; 3, 100 000 × *g* supernatant of solubilized liver mitochondria; 4, final resin wash in 10 mM Hepes (pH 6.90), 1 mM EDTA; 5, resin elution using 50 μmol CMP; 6, non-specific elution with 0.8 M NaCl; 7, molecular mass markers. Based on migration of the markers (provided on right), molecular masses of UCP1 and UCP2 were calculated to be 32.7 and 37.4 kDa, respectively. Recombinant UCP2 contains an additional 17 amino acids (11 at the N-terminus and 6 at the C-terminus) that is predicted to add 2.2 kDa to its mass. Theoretical molecular masses of UCP1 and UCP2 are 33.1 and 33.2 kDa, respectively. Two proteins recovered from the eluted resin which are similar in size to UCP1 and UCP2 were calculated to have relative molecular masses of 31.2 and 32.6 kDa.

true for liver but not for muscle mitochondria. Pre-incubation of liver mitochondria with CMP more than doubled basal respiration while not significantly affecting the maximal FCCP-stimulated respiration. In muscle, basal respiration with CMP was significantly greater than that with the other nucleotides tested, but did not differ from that without nucleotide (Fig. 4B). In both types of mitochondria AMP

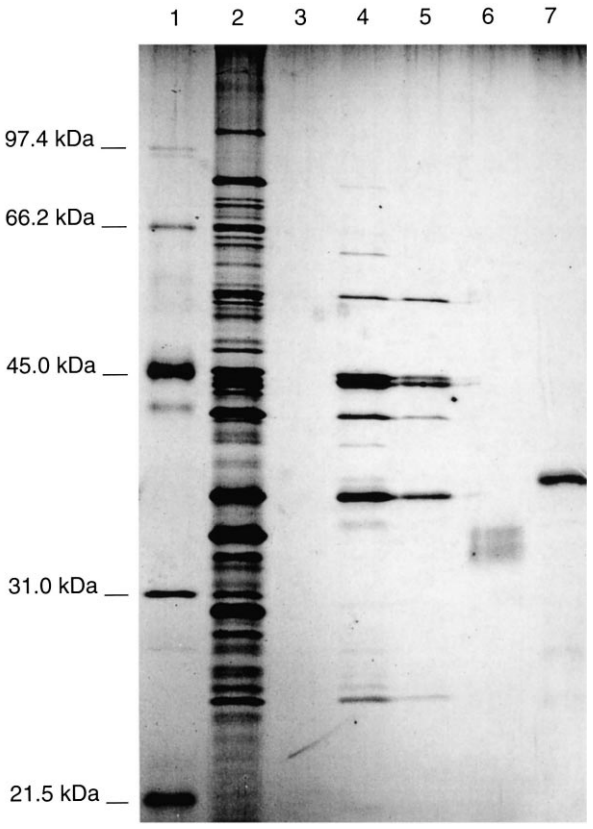

Fig. 8. SDS–PAGE analysis of solubilized skeletal muscle mitochondrial proteins prior to and following batch CMP-agarose chromatography. Isolated skeletal muscle mitochondria were processed as described in Fig. 7 except that the resin was washed ten times under slightly less stringent conditions. Lanes: 1, molecular mass markers; 2, 100 000 × *g* supernatant of solubilized skeletal muscle mitochondria; 3, final resin wash with 10 mM Hepes (pH 6.90), 1 mM EDTA; 4, resin elution using 50 μmol CMP; 5, non-specific elution using 0.8 M NaCl; 6, rat UCP1; 7, recombinant human UCP2. Based on migration of the markers (provided on right), molecular masses of UCP1 and UCP2 were calculated to be 33.7 and 38.7 kDa, respectively. Recombinant UCP2 contains an additional 17 amino acids (11 at the N-terminus and 6 at the C-terminus) that is predicted to add 2.2 kDa to its mass. The two proteins closest in size to UCP1 and UCP2 had relative molecular masses of 35.0 and 37.2 kDa.

and GDP had little effect on basal respiration but significantly reduced the effect of FCCP. We also tested 2′-deoxythymidine 5′-monophosphate (TMP) to determine if a different pyrimidine monophosphate had effects similar to CMP. This was not the case, as TMP significantly increased liver RCR and tended to increase muscle RCR.

3.3. Nucleotide effects on mitochondrial swelling

To further investigate the effect of CMP, inner mitochondrial membrane proton permeabilities were assessed by measuring initial swelling rates of non-respiring mitochondria. Increasing membrane proton permeability with titrations of FCCP produced significant changes in liver (not shown) and skeletal muscle mitochondrial swelling rates (Fig. 1). Increasing concentrations of CMP also stimulated both liver and muscle mitochondrial swelling (Fig. 5). At the highest concentration tested, CMP-stimulated swelling was 45% and 33% of that induced by 0.5 μM FCCP in liver and muscle, respectively.

In these experiments, CMP was added as a sodium salt containing 2 mol sodium per mol nucleotide, whereas AMP contained 1 mol sodium per mol nucleotide. To preclude the possibility that the differences between CMP and AMP were the result of differences in the amount of sodium added into the swelling buffer, control experiments were performed in which the amount of sodium was adjusted in the AMP stock to equal that of the CMP stock. Even with the additional sodium, AMP did not stimulate swelling of either liver or skeletal muscle mitochondria; in fact, mitochondria tended to shrink (as indicated by an initial increase in absorbance units after addition) as a result of the additional osmotic load (data not shown).

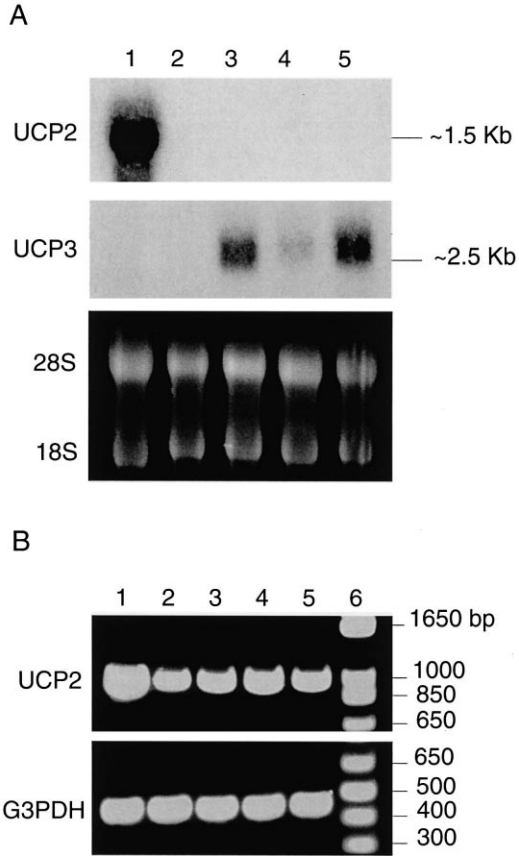

Fig. 9. Expression profiles of UCP2 and UCP3 in lean Zucker rat liver and skeletal muscle assessed by Northern blot (A) and RT–PCR (B). Northern blotting and RT–PCR was performed as described in Section 2. (A) Lanes: 1, spleen; 2, liver; 3, gastrocnemius; 4, soleus; 5, tibialis anterior. Approximate sizes of the signals, in kilobase pairs (Kb), are indicated on the right. Ethidium bromide staining of 28S and 18S RNA is provided for verifying equal RNA loading. A 2-day exposure of the blot at −80°C with intensifying screen was sufficient to detect UCP3 in muscle but not UCP2 in liver or muscle. Lanes in B are as in A, except that lane 6 is a molecular mass ladder, in base pairs (bp). Amplification of glyceraldehyde 3-phosphate dehydrogenase (G3PDH) served as positive control for RT–PCR reactions.

3.4. Nucleotide effects on proton leak kinetics

Following pre-incubation with CMP, TMP, or no nucleotide, oligomycin-treated and succinate-energized mitochondria were titrated with malonate (a competitive inhibitor of succinate dehydrogenase) so that changes in $\Delta\Psi$ via TPMP distribution could be determined as respiration progressively slowed. In this way the respiration required to sustain a given $\Delta\Psi$ could be determined. In the presence of CMP, liver but not muscle mitochondria required a greater respiration rate to sustain a given $\Delta\Psi$ (Fig. 6). After linear transformation of the data, analysis of covariance revealed no significant main effect of nucleotide on the slopes in either tissue ($0.1 < P < 0.05$). However, a Tukey post hoc test revealed that, in liver, the slope with CMP differed significantly from that with TMP or no addition. In muscle, neither the CMP nor the TMP slopes were significantly different from the control slope.

3.5. CMP–agarose chromatography

Because our results consistently showed a CMP effect in liver but not muscle, we wanted to determine if liver mitochondria contain a CMP-binding protein that is absent from muscle mitochondria. Isolated liver and skeletal muscle mitochondria from two fasted rats were solubilized for 45 min in our standard reaction buffer containing 4% Triton X-100. The solubilized proteins were incubated overnight with CMP–agarose, which was then washed extensively and subjected to a CMP elution. Two proteins of particular interest that were eluted from liver but not muscle (despite using less stringent washing of the muscle preparations) had relative molecular masses of 31.2 and 32.6 kDa (Figs. 7 and 8). To determine the protein remaining following the CMP elution, the resin was treated with 0.8 M NaCl at pH 8. No unique bands (vs. CMP treatment) were obtained, indicating that the resin was washed sufficiently to remove any non-specifically bound proteins.

3.6. UCP2 and UCP3 expression

Expression of liver and spleen UCP2, and muscle UCP2 and UCP3 were determined in our lean Zucker rat colony to verify that this strain expresses these genes in a manner similar to other rat strains. UCP2 was not detected in liver or muscle after exposing Northern blots for 2 days to X-ray film with intensifying screen (Fig. 9). Using the same exposure, a UCP3 signal was detected in gastrocnemius, soleus, and tibialis anterior. Liver and muscle UCP2 signals were obtained by RT–PCR (Fig. 9B).

4. Discussion

The primary objective of this study was to test the hypothesis that adenine nucleotide tri- and diphosphates inhibit basal liver and skeletal muscle mitochondrial proton leak. Our data negate this hypothesis. ATP and ADP (as well as CTP) inhibited respiration and fluorescence, indicating that these nucleotides inhibited one or more components of the respiratory chain. Additionally, GTP and GDP did not significantly affect liver respiration and had small, albeit significant, inhibitory effects on muscle respiration. We chose to conduct most of these experiments at a relatively non-physiological pH of 6.9, similar to other studies with UCP2 and UCP3 [4–7,16], because UCP1 binds nucleotides more effectively under acidic conditions [17]. Thus, if nucleotides were to have an effect on proton leak via inhibition of UCP2 and UCP3, the effect should be more obvious at lower pHs.

Our results, together with recent findings [8,18], suggest that the basal proton leak common in mitochondria from many different tissues is not inhibited by purine nucleotides. One interpretation of these data is that UCP2 and UCP3 do not mediate the basal proton leak in mammalian mitochondria. This interpretation is valid if the purine nucleotide-sensitive activities of reconstituted UCP2 and UCP3 measured by Jaburek et al. [3] and Echtay et al. [4] accurately reflect that which occurs in isolated mitochondria. The possibility that UCP2 and UCP3 are inactive in isolated mitochondria [7,16,19] could explain why purine nucleotides do not inhibit proton leak. If this were true, the conclusion must be that these proteins do not mediate the basal leak observed in isolated mitochondria. However, since Zhang et al. [7], Hinz et al. [5], and Rial et al. [6] did not find purine nucleotide-sensitive uncoupling in isolated yeast mitochondria expressing recombinant UCP2 and UCP3, the alternative interpretation of our data is that effects of purine nucleotides cannot be used as a valid means of determining if UCP2 and UCP3 mediate basal proton leak.

In these experiments BSA was neither included in the isolation buffer nor in the reaction medium. Consequently, fatty acids, which are potential cofactors necessary for reconstituted UCP2 and UCP3 activity [3], were certainly present in our preparations (albeit at unknown levels). The possibility that the endogenous fatty acids were depleted via β-oxidation within the mitochondrial matrix during the 6–8-min preincubations at 37°C is extremely unlikely because respiration was negligible during this period. Moreover, the reaction buffer contained rotenone to eliminate any NADH-linked substrate oxidation, and lacked carnitine, which is required for fatty acid transport into the matrix. Therefore, the fact that we did not observe an effect of purine nucleotides on proton leak is unlikely to be due to

the absence of fatty acids in our mitochondrial preparations.

We did find a pyrimidine nucleotide-inducible leak in liver mitochondria. At 12 mM CMP, proton leak was about 2.5 times greater than without nucleotide (Fig. 6) and basal respiration was increased to 71% of that caused by the ohmic uncoupler FCCP (Fig. 4). Because the concentration of CMP required to stimulate the leak far exceeds the physiological range for pyrimidine nucleotide monophosphates [20], CMP cannot be considered a physiologically important regulator. Nonetheless, we do not believe that CMP acts in a non-specific manner because (a) the effect is not observed in skeletal muscle mitochondria; (b) within the same concentration range, none of the other nucleotides tested had the same affect; (c) the effect was reduced at pH 7.65; and (d) there were proteins recovered from liver mitochondria by CMP chromatography that were not recovered from muscle mitochondria, where CMP did not affect the leak kinetics. The importance of this finding resides in the fact that we have found a non-fatty acid compound that acutely activates a leak in a tissue other than BAT. This raises the possibility that there are physiologically relevant intracellular factors which regulate mitochondrial proton leak and, potentially, resting metabolism.

Further experiments are necessary to determine if the proteins isolated from liver mitochondria that are similar in size to UCPs and other members of the mitochondrial carrier protein family are responsible for the CMP-inducible leak. Although UCP2 is expressed in lean Zucker rat liver (Fig. 9), CMP is unlikely to act via this protein because it is also present in muscle (Fig. 9), where the leak is not affected by CMP. Moreover, because UCP2 is only weakly expressed in liver due to its apparent absence in parenchymal hepatocytes [21], the pronounced uncoupling effect of CMP likely involves a protein that has greater abundance in this tissue. This raises the possibility that liver mitochondria express a protein with uncoupling activity that is not expressed in muscle mitochondria.

Since UCP1 homologs are up-regulated in certain tissues by fasting [22–26], we fasted our rats prior to attempting protein isolation using CMP–agarose. It should be emphasized that the leak mechanism induced by CMP may be entirely different from that of the basal leak; our data provide no evidence about the mechanism that causes the basal leak in liver or muscle, other than it is insensitive to nucleotides such as ATP and CTP.

Mitochondrial swelling is used as an index of inner mitochondrial membrane proton permeability. We found that CMP did stimulate muscle mitochondrial swelling despite the fact that it did not significantly stimulate non-phosphorylating respiration or the kinetics of the leak in this tissue. This discrepancy may be related to the fact that swelling was measured in non-energized mitochondria while all other experiments were conducted with mitochondria oxidizing succinate. Since proton pumping by the respiratory chain does not 'slip' (i.e., reduced H^+/O) at high $\Delta\Psi$ [27], Fig. 6 illustrates that the magnitude of the leak is dependent upon the inner mitochondrial membrane potential. Under non-phosphorylating conditions, energized mitochondria generate a maximal membrane potential-driven leak. This leak may be sufficient to mask any small CMP-mediated effect. We did obtain different proteins from muscle vs. liver mitochondria via CMP chromatography, albeit under slightly less stringent conditions than that used for liver. Thus, we cannot rule out the possibility that CMP does affect the inner membrane proton permeability of muscle mitochondria under certain conditions.

Dose-dependent inhibition of respiration and fluorescence by ATP and CTP indicates that these nucleotides inhibit the electron transport system. The fact that ATP had the same effect in the presence of atractyloside indicates that it did not inhibit respiration by acting within the mitochondrial matrix. Proteins which hydrolyze a nucleotide triphosphate to drive their catalytic activities (e.g., kinases) typically require Mg to be complexed with the triphosphate. In contrast, Mg-free nucleotides are the preferred ligand for enzymes that are allosterically regulated by nucleotides. Removing Mg from the reaction buffer significantly increased the inhibitory effects of ATP, suggesting that it did not act as substrate for a kinase. Moreover, these data negate the hypothesis that the inhibitory effects of ATP (and probably CTP) are an indirect result of Mg removal from the buffer by chelation with the triphosphate. Taken together, these data suggest that ATP allosterically inhibits respiratory chain activity via a bind-

ing site which faces the cytosol. This site is not on complex I of the respiratory chain because rotenone was present to block all NADH linked oxidation. Since CTP is not used by kinases in phosphorylating reactions, it may be acting in a manner similar to that of ATP.

Cytosolic oriented, low-affinity (i.e., millimolar range) binding sites for ATP have been reported to exist on cytochrome *c* [28,29] and cytochrome *c* oxidase [30]. Based on experiments using the isolated or reconstituted proteins, cytosolic ATP levels have been proposed to play a physiologically relevant role in allosterically inhibiting electron transport through these enzymes [29,30]. Matrix ATP binding sites on cytochrome *c* oxidase have also been suggested as important in regulating electron transport chain activity [31–33]. Our data with isolated mitochondria suggest that one or more low-affinity cytosolic sites for ATP may control respiratory chain activity. However, an intracellular pH of 6.9 represents an acidic condition likely to occur in vivo only during exercise or ischemia [34]. Under such conditions, ATP levels fall below their resting concentrations, which in rat liver has been reported to be 6.2 mM [35]; thus, the IC_{50} values obtained do not reflect the intracellular ATP levels which would be present in vivo at pH 6.9. Nonetheless, the cytosolic concentration of Mg during high metabolic activity is a potentially important factor dictating the efficacy of ATP. Further studies at a pH of 7.1–7.2 are required to determine the concentration of ATP necessary to regulate respiratory chain activity during periods of relatively low metabolic activity. Regardless of pH, the physiological significance of respiratory inhibition by CTP is questionable given that it is typically present at concentrations one to two orders of magnitude less than the calculated IC_{50} value.

In summary, liver mitochondrial proton leak is activated by non-physiological concentrations of cytidine 5′-monophosphate. Energized muscle mitochondria were not affected by CMP. The CMP-inducible leak in liver may be mediated by proteins with relative molecular masses of 31.2 and/or 32.6 kDa. In liver and muscle, ATP and CTP inhibit electron transport at a pH- and Mg-sensitive cytosolic site. Given the concentrations required to achieve inhibition, ATP is the only nucleotide with potential physiological relevance.

Acknowledgements

This research was supported in part by NIH Grants DK32907, DK35747, and T32-HL-07682. We thank Dr John Crowe for use of the fluorescence spectrophotometer, John Horowitz and Jock Hamilton for technical assistance, Francine Gregoire and Lina Kwong for UCP expression data, and Sue Bennett for breeding and care of the rats.

References

[1] D.G. Nicholls, R.M. Locke, Thermogenic mechanisms in brown fat, Physiol. Rev. 64 (1984) 1–64.
[2] M.D. Brand, K.M. Brindle, J.A. Buckingham, J.A. Harper, D.F. Rolfe, J.A. Stuart, The significance and mechanism of mitochondrial proton conductance, Int. J. Obes. Relat. Metab. Disord. 23 (Suppl 6) (1999) S4–11.
[3] M. Jaburek, M. Varecha, R.E. Gimeno, M. Dembski, P. Jezek, M. Zhang, P. Burn, L.A. Tartaglia, K.D. Garlid, Transport function and regulation of mitochondrial uncoupling proteins 2 and 3, J. Biol. Chem. 274 (1999) 26003–26007.
[4] K.S. Echtay, Q. Liu, T. Caskey, E. Winkler, K. Frischmuth, M. Bienengraber, M. Klingenberg, Regulation of UCP3 by nucleotides is different from regulation of UCP1, FEBS Lett. 450 (1999) 8–12.
[5] W. Hinz, S. Gruninger, A. De Pover, M. Chiesi, Properties of the human long and short isoforms of the uncoupling protein-3 expressed in yeast cells, FEBS Lett. 462 (1999) 411–415.
[6] E. Rial, M. Gonzalez-Barroso, C. Fleury, S. Iturrizaga, D. Sanchis, J. Jimenez-Jimenez, D. Ricquier, M. Goubern, F. Bouillaud, Retinoids activate proton transport by the uncoupling proteins UCP1 and UCP2, EMBO J. 18 (1999) 5827–5833.
[7] C.Y. Zhang, T. Hagen, V.K. Mootha, L.J. Slieker, B.B. Lowell, Assessment of uncoupling activity of uncoupling protein 3 using a yeast heterologous expression system, FEBS Lett. 449 (1999) 129–134.
[8] S. Monemdjou, L.P. Kozak, M.E. Harper, Mitochondrial proton leak in brown adipose tissue mitochondria of Ucp1-deficient mice is GDP insensitive, Am. J. Physiol. 276 (1999) E1073–E1082.
[9] S. Cadenas, J.A. Buckingham, S. Samec, J. Seydoux, N. Din, A.G. Dulloo, M.D. Brand, UCP2 and UCP3 rise in starved rat skeletal muscle but mitochondrial proton conductance is unchanged, FEBS Lett. 462 (1999) 257–260.
[10] P.L. Altman, D.S. Dittmers (Eds.), Biological Handbook Series: Respiration and Circulation, Federation of American Societies for Experimental Biology, Bethesda, MD, 1971, p. 18.
[11] A. Cossarizza, D. Ceccarelli, A. Masini, Functional hetero-

geneity of an isolated mitochondrial population revealed by cytofluorometric analysis at the single organelle level, Exp. Cell Res. 222 (1996) 84–94.
[12] M.D. Brand, Measurement of mitochondrial protonmotive force, in: G.C. Brown, C.E. Coopers (Eds.), Bioenergetics, A Practical Approach, Oxford University Press, New York, 1995, pp. 39–62.
[13] R.P. Hafner, C.D. Nobes, A.D. McGown, M.D. Brand, Altered relationship between protonmotive force and respiration rate in non-phosphorylating liver mitochondria isolated from rats of different thyroid hormone status, Eur. J. Biochem. 178 (1988) 511–518.
[14] D.G. Nicholls, E. Rial, Measurement of proton leakage across mitochondrial inner membranes and its relation to protonmotive force, Methods Enzymol. 174 (1989) 85–94.
[15] D.G. Nicholls, The bioenergetics of brown adipose tissue mitochondria, FEBS Lett. 61 (1976) 103–110.
[16] T. Hagen, C.Y. Zhang, C.R. Vianna, B.B. Lowell, Uncoupling proteins 1 and 3 are regulated differently, Biochemistry 39 (2000) 5845–5851.
[17] M. Klingenberg, Nucleotide binding to uncoupling protein. Mechanism of control by protonation, Biochemistry 27 (1988) 781–791.
[18] S. Cadenas, M.D. Brand, Effects of magnesium and nucleotides on the proton conductance of rat skeletal-muscle mitochondria, Biochem. J. 348 (Pt. 1) (2000) 209–213.
[19] M.B. Jekabsons, F.M. Gregoire, N.A. Schonfeld-Warden, C.H. Warden, B.A. Horwitz, T(3) stimulates resting metabolism and UCP-2 and UCP-3 mRNA but not nonphosphorylating mitochondrial respiration in mice, Am. J. Physiol. 277 (1999) E380–E389.
[20] M.E. Jones, Pyrimidine nucleotide biosynthesis in animals: genes, enzymes, and regulation of UMP biosynthesis, Annu. Rev. Biochem. 49 (1980) 253–279.
[21] D. Larrouy, P. Laharrague, G. Carrera, N. Viguerie-Bascands, C. Levi-Meyrueis, C. Fleury, C. Pecqueur, M. Nibbelink, M. Andre, L. Casteilla, D. Ricquier, Kupffer cells are a dominant site of uncoupling protein 2 expression in rat liver, Biochem. Biophys. Res. Commun. 235 (1997) 760–764.
[22] D.W. Gong, Y. He, M. Karas, M. Reitman, Uncoupling protein-3 is a mediator of thermogenesis regulated by thyroid hormone, beta3-adrenergic agonists, and leptin, J. Biol. Chem. 272 (1997) 24129–24132.
[23] O. Boss, S. Samec, A. Dulloo, J. Seydoux, P. Muzzin, J.P. Giacobino, Tissue-dependent upregulation of rat uncoupling protein-2 expression in response to fasting or cold, FEBS Lett. 412 (1997) 111–114.
[24] S. Samec, J. Seydoux, A.G. Dulloo, Interorgan signaling between adipose tissue metabolism and skeletal muscle uncoupling protein homologs: is there a role for circulating free fatty acids?, Diabetes 47 (1998) 1693–1698.
[25] O. Boss, S. Samec, F. Kuhne, P. Bijlenga, F. Assimacopoulos-Jeannet, J. Seydoux, J.P. Giacobino, P. Muzzin, Uncoupling protein-3 expression in rodent skeletal muscle is modulated by food intake but not by changes in environmental temperature, J. Biol. Chem. 273 (1998) 5–8.
[26] S. Samec, J. Seydoux, A.G. Dulloo, Role of UCP homologues in skeletal muscles and brown adipose tissue: mediators of thermogenesis or regulators of lipids as fuel substrate?, FASEB J. 12 (1998) 715–724.
[27] M.D. Brand, L.F. Chien, P. Diolez, Experimental discrimination between proton leak and redox slip during mitochondrial electron transport, Biochem. J. 297 (1994) 27–29.
[28] D.B. Craig, C.J. Wallace, The specificity and K_d at physiological ionic strength of an ATP-binding site on cytochrome *c* suit it to a regulatory role, Biochem. J. 279 (1991) 781–786.
[29] D.B. Craig, C.J. Wallace, ATP binding to cytochrome *c* diminishes electron flow in the mitochondrial respiratory pathway, Protein Sci. 2 (1993) 966–976.
[30] J.W. Taanman, P. Turina, R.A. Capaldi, Regulation of cytochrome *c* oxidase by interaction of ATP at two binding sites, one on subunit VIa, Biochemistry 33 (1994) 11833–11841.
[31] B. Kadenbach, S. Arnold, A second mechanism of respiratory control, FEBS Lett. 447 (1999) 131–134.
[32] B. Kadenbach, J. Napiwotzki, V. Frank, S. Arnold, S. Exner, M. Huttemann, Regulation of energy transduction and electron transfer in cytochrome *c* oxidase by adenine nucleotides, J. Bioenerg. Biomembr. 30 (1998) 25–33.
[33] S. Arnold, B. Kadenbach, The intramitochondrial ATP/ADP-ratio controls cytochrome *c* oxidase activity allosterically, FEBS Lett. 443 (1999) 105–108.
[34] S. Sunoo, K. Asano, F. Mitsumori, ^{31}P nuclear magnetic resonance study on changes in phosphocreatine and the intracellular pH in rat skeletal muscle during exercise at various inspired oxygen contents, Eur. J. Appl. Physiol. 74 (1996) 305–310.
[35] W.D. Schwenke, S. Soboll, H.J. Seitz, H. Sies, Mitochondrial and cytosolic ATP/ADP ratios in rat liver in vivo, Biochem. J. 200 (1981) 405–408.